THESEUS and quasar microlensing

Lindita Hamolli, Mimoza Hafizi*

Department of Physics, University of Tirana, Albania; lindita.hamolli@fshn.edu.al

Abstract: Quasar microlensing is called the lensing effect on quasars, caused by compact objects in the mass range $[10^{-6}, 10^{3}]M_{O}$, inside a lens galaxy. It is shown that quasar microlensing provides a possibility to probe extragalactic planets in the lens galaxy. THESEUS will observe with a unique combination of huge FOV, angular resolution and sensitivity. We focus on the ability of THESEUS to probe, through quasar microlensing, extragalactic planets.

Keywords: Gravitational Lensing, Strong Lensing, Weak Lensing, Microlensing, Quasar Microlensing

1. Introduction

Quasars are the most luminous, powerful, and energetic objects known in the universe. They can be gravitationally lensed by a foreground galaxy, which deflects the light rays, when is close to the line of sight. In 1916, Einstein calculated the light deflection by the Sun, based on the general theory of relativity [1] and found the value $\alpha = 4GM / bc^2$, twice more than the previous value found, based on Newtonian mechanics [2]. Here G is the gravitational constant, M is the lens's mass and b is the impact parameter of the light rays. The general relativistic result was confirmed during the Solar eclipse in 1919 [3]. In 1936, Einstein published a paper describing the gravitational lensing effect caused by distant stars, considering the particular case when the source, the lens and the observer are aligned. He noticed the existence of a luminous ring, after called the Einstein ring [4], hopelessly to be observed at that epoch. In 1937, Zwicky understood that galaxies were gravitational lenses more powerful than stars and might give rise to images with a detectable angular separation [5].

Actually, there are different scales in gravitational lensing. The strong (or macro) lensing is the regime when the gravitational lens images are separated by more than a few tenths of arcsecs and can be observed as distinct images. In the case when the distortions induced by the gravitational fields are much smaller, we have the weak lensing effect. On the other side, if one considers the star-on-star lensing (as Einstein did), the resulting angular distance between the images is of the order of *mas*, generally not separable by telescopes. Gravitational lensing in this regime is called microlensing and the observable is an achromatic change in the brightness of the source star over time, due to the relative motion of the lens with respect to the line of sight towards the source [6]. Recently, a new effect, quasar microlensing, is detected inside the images obtained during the strong lensing, which is related to the uncorrelated brightness fluctuations of the macro-images due to the motion of the deflectors (the constituting objects of the lensing galaxy). By this effect, it becomes possible to constrain the fraction of free floating planets (FFPs) in other galaxies [7].

The first attempts to characterize the free floating planet population in our Galaxy were done by Sumi et al. [9], by analyzing the microlensing light curves of two-year survey of

MOA-II collaboration towards the Galactic bulge. They reported the discovery of planetary-mass objects (the mass rang $[10^{-5}, 10^{-2}]M_{\odot}$) either very distant from their host star ($\sim 100\ AU$) or entirely unbound. By the best-fit procedure of the observed microlensing events due to FFPs, they constrained a power-law mass function with the index $\alpha_{PL} = 1.3^{+0.3}_{-0.4}$ and defined the number of planetary mass objects per star: $N_{PL} = 5.5^{+18.1}_{-4.3}$. Current microlensing observations are performed by the ground-based telescopes OGLE [9] and MOA [10] and by the space-based telescopes Kepler [11] and Spitzer [12]. In recent years, FFPs are found in many young star forming regions by using infrared imaging surveys [13]. The origin of the FFPs is uncertain. One possibility is that they originally formed around a host star and then scattered out from orbit. A second option is that they may form on their own through gas cloud collapse, similarly to star formation.

The Transient High Energy Sky and Early Universe Surveyor (THESEUS) is a space mission concept developed by a large international collaboration, in response to the calls for M-class missions by the European Space Agency (ESA) [14]. Apart from GRBs, THESEUS will observe Quasars and AGN-s in very large distances. We discuss here about the ability of THESEUS to probe, by this way, extragalactic planets.

In the next section, we review the basics of gravitational lensing, in its regimes: strong lensing, weak lensing and microlensing. In Section 3 we discuss quasar microlensing following by description of THESEUS mission capabilities in Section 4. Our conclusions are given in Section 5.

2. Basics of Gravitational Lensing

In the general theory of relativity, light rays follow null geodesics, i.e., the minimum distance paths in a curved space-time. Therefore, when a light ray from a far source interacts with the gravitational field due to a massive body, it is bent by an angle $\alpha = 4GM / bc^2$. By looking at Figure 1, assuming the ideal case of a thin lens and noting that, $\alpha D_{LS} = (\theta - \theta_S)D_S$ one can easily derive the so-called lens equation

$$\theta\text{-}\theta_S = \theta_E^2/\theta \tag{1}$$

where θ_S indicates the source position and

$$\theta_E = \sqrt{\frac{4GM}{c^2}\frac{D_{LS}}{D_L D_S}} \tag{2}$$

is the Einstein ring radius, which is the angular radius of the image when the lens and the source are perfectly aligned, $\theta_S=0$. Here, D_S, D_L and D_{LS} are the angular diameter distances between the observer, lens, and source, respectively. By solving Equation (1), one can define the positions of two images appeared in the source plane. More generally, the light deflection between the two-dimensional position of the source θ_S and that of the position of the image θ is given by the lens mapping equation [15]:

$$\theta_S = \theta - \nabla\varphi(\theta) \tag{3}$$

where φ is the so-called lensing potential of the lens. Eqn. 3 is a transformation from the source plane to the image plane. The Jacobian of the transformation is given by:

$$J = \frac{d\theta_S}{d\theta} = A^{-1} = \begin{pmatrix} 1-\varphi_{,11} & -\varphi_{,12} \\ -\varphi_{,12} & 1-\varphi_{,22} \end{pmatrix} = \begin{pmatrix} 1-\kappa-\gamma_1 & -\gamma_2 \\ -\gamma_2 & 1-\kappa+\gamma_1 \end{pmatrix} \quad (4)$$

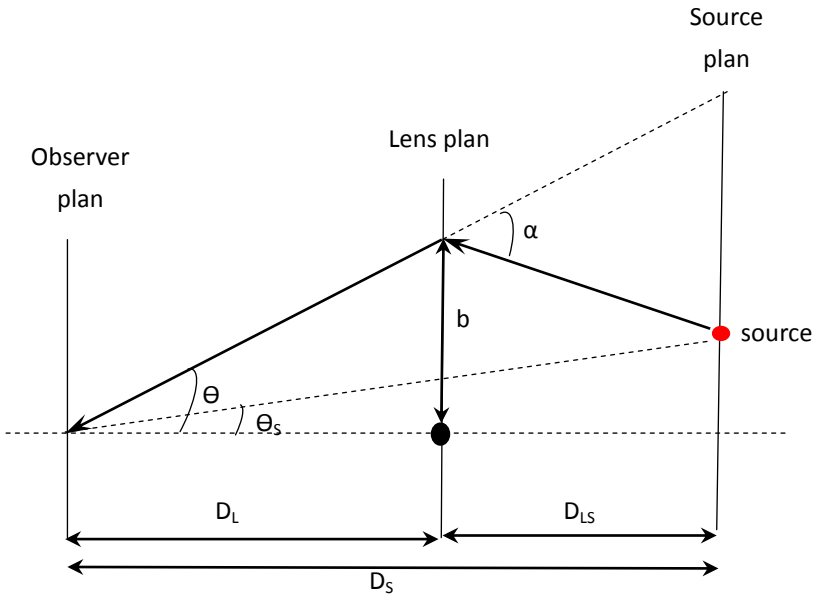

Fig1 *. Schematics of the lensing phenomenon.*

where the commas are the partial derivatives with respect to the two components of θ, A is named magnification matrix, k - convergence and γ - shear. The points in the source plane where A=0 form the so called caustic lines.

The optical depth τ is defined as the fraction of a given solid angle $\delta\Omega$ covered by the Einstein rings of the individual masses. To first order, it is equal to the convergence, or normalized surface mass density

$$\tau = \sum_i \frac{(\pi\theta_E^2)_i}{\delta\Omega} = \frac{\Sigma}{\Sigma_{crit}} = \kappa \quad (5)$$

where the critical density is $\Sigma_{crit} = \frac{c^2 D_S}{4\pi G D_L D_{LS}}$.

2.1. Strong lensing

The strong gravitational lensing was first observed in 1979 and was linked to a quasar (QSO 0957+561) [16]. The existence of two objects separated by about 6″ and characterized by an identical spectrum led to the conclusion that they were the doubled image of the same quasar. This double quasar was also the first object for which the time delay (about 420 days) between the two images [17], due to the different paths of the photons, has been measured. Observations can also show four images of the same quasar, as in the case of the so-called Einstein Cross, or when the lens and the source are closely aligned, one can observe the Einstein ring, as in the case of MG 1131+0456 [18]. The sources of strong lensing events are

often quasars, galaxies, galaxy clusters and supernovae, whereas the lenses are usually galaxies or galaxy clusters. The image separation is generally larger than a few tenths of an arcsec, often up to a few arcsecs. Over the years, many strong lensing events have been found in deep surveys of the sky, such as the CLASS [19], the Sloan ACS [20], the SQLS (the Sloan Digital Sky Survey for Quasar Lens Search) [21], and so on.

Strong gravitational lensing is nowadays a powerful tool for investigation in astrophysics and cosmology. It may be used as a natural telescope that magnifies dim galaxies, making them easier to be studied in detail [22].

2.2. Weak lensing

In addition to the macroscopic deformations, in the deep field surveys of the sky single distorted images with elliptical shape and weakly distorted images of galaxies have been also detected. This effect is known as weak lensing and is playing an increasingly important role in cosmology. The first weak lensing event was detected in 1990 as statistical tangential alignment of galaxies behind massive clusters [23], but only in 2000, coherent galaxy distortions were measured. The weak lensing cannot be measured by a single galaxy, but its observation relies on the statistical analysis of the shape and alignment of a large number of galaxies in a certain direction.

2.3. Microlensing

The lensing phenomenon is called microlensing when θ_E is much smaller than the typical telescope angular resolution, as in the case of stars lensing the light from background stars. In the simplest case, when the point-like approximation for both lens and source is assumed and the relative motion among the observer, lens and source are uniform and linear, individual images cannot be resolved due to their small separation, but the total brightness of the images is larger with respect to that of the unlensed source, leading to a specific time dependent amplification of the source [5], which is given by,

$$A = \frac{2+u^2}{u\sqrt{4+u^2}} \geq 1. \tag{6}$$

where $u = \theta_S / \theta_E$. The parameter u can be decomposed into components parallel and perpendicular to the direction of the relative lens-source motion and be calculated as

$$u(t) = \sqrt{\frac{(t-t_0)^2}{t_E} + u_0^2} \tag{7}$$

where t_0 and u_0 are the time and impact parameter at the closest-approach. The Einstein time scale $t_E = R_E / v_T$ is defined as the time required for the lens to traverse the Einstein radius (R_E). The light curve is determined by three parameters: t_0, t_E and u_0. However, of these parameters only t_E contains information about the lens and this gives rise to the so-called parameter degeneracy problem. To break this degeneracy, the second order effects are considered, which are: the parallax effect ([24]-[26]), the finite source effects ([27], [28]) and the binary lens effect [29]. A microlensing event can also be observed astrometrically and the elliptic trajectory of the centroid can be detected, which depends on the angular Einstein radius ([30]-[32]).

3. Quasar Microlensing

The quasars can be affected by gravitational lensing in two ways. The "Macrolensing" concerns multiply imaged quasars, with angular separations of roughly an arcsecond. These cases are produced by typical galaxy lenses with masses of the order of $10^{12}M_{\odot}$. About one out of 500 quasars is multiply imaged [33]. Some hundred of cases are known to date, most of them consist of double or quadruple images. The second interesting regime is "microlensing": the compact objects in the mass range $[10^{-6}, 10^{3}]M_{\odot}$ affect the apparent brightness of the quasar images. The microlenses can be ordinary stars, brown dwarfs, planets, black holes, molecular clouds, globular clusters or other compact mass concentrations. In most practical cases, the microlenses are part of a galaxy which acts as the main (macro-)lens. The brightness fluctuations on the macro-images can be used to study the size and brightness profile of quasars on one hand, and the distribution of compact (dark) matter along the line of sight on the other hand.

In strong lensing regime of the quasar, for massive galaxy with mass of $M=10^{12}M_{\odot}$ at a redshift $z_L = 0.5$ and a source at redshift $z_S=2.0$ (here $H_0 = 50\ km\ s^{-1}Mpc^{-1}$) the Einstein radius is

$$\theta_E \approx 1.8\sqrt{\frac{M}{10^{12}M_{\odot}}}\ \text{arcsec.} \tag{8}$$

For a quasar microlensing scenario in which stars in the lensing galaxy act as a lens for a background quasar, the scale defined by the Einstein radius is

$$\theta_E \approx 10^{-6}\sqrt{\frac{M}{M_{\odot}}}\ \text{arcsec.} \tag{9}$$

This corresponds to a physical scale (Einstein radius in source plan)

$$r_E \approx 1.4x10^{16}\sqrt{\frac{M}{M_{\odot}}}\ \text{cm.} \tag{10}$$

Quasar microlensing happens to be an interesting phenomenon when the size of the optical continuum emitting region of the quasars is comparable to or smaller than the Einstein radius of stellar mass objects. In fact, the image splittings on such angular scales cannot be observed directly, but the microlensing can be observable because the observer, lens(es) and source move relative to each other and the micro-image configuration changes with time. This fluctuation in magnification can be measured and used to study the quasars and the distribution of compact (dark) matter along the line of sight. In these events, two time scales can be defined. The standard lensing time scale t_E is the time the source takes to cross the Einstein radius of the lens

$$t_E = \frac{r_E}{v_{\perp,eff}} \approx 15\sqrt{M/M_{\odot}}\, v_{600}^{-1}\ years \tag{11}$$

where the effective relative transverse velocity $v_{\perp,eff}$ is parametrized in units of 600 km/s: v_{600}. This time scale t_E results in large pessimistically observable values. However, in practice we can expect fluctuations on much shorter time intervals. The reason is that sharp caustic lines separate regions of low and high magnification. Hence, if the source crosses such a caustic line, we can observe a large change in magnification within the crossing time t_{cross} , which is the

time needed for the source to cross its own radius R_{source}:

$$t_{cross} = \frac{R_{source}}{v_{\perp,eff}} \approx 4R_{15}v_{600}^{-1}\ months \quad (12)$$

Here the quasar size R_{15} is parametrized in units of 10^{15} cm.

As shown above, the fluctuations in the brightness of a quasar can have two causes: intrinsic to the quasar, or induced by microlensing. In the case when there are two or more macro-lensing images of a quasar, it is possible to distinguish between two possible causes of variability: any fluctuations caused by intrinsic variability of the quasar show up in all quasar images, with a time-lag according to the time delay. So, once a time delay is measured in a multiply-imaged quasar system, one can "shift" the light curves of the different quasar images relative to each other by the time delay, correct for the different (macro-)magnification (due to the smooth lensing galaxy mass model), and subtract them from each other. All remaining incoherent fluctuations in this "difference light curve" can be attributed to microlensing.

Recently, the Chandra observations of several gravitationally lensed quasars show evidence for flux and spectral variability of the X-ray emission that is uncorrelated between images and is thought to result from the microlensing by stars in the lensing galaxy.

Dai & Guerras [7] found that in the lens galaxy there are ~ 2000 objects per main sequence star in the mass range between Moon and Jupiter.

4. THESEUS

The Transient High Energy Sky and Early Universe Surveyor (THESEUS) is a space mission concept developed by a large international collaboration, aimed at finding answers to multiple fundamental questions of modern cosmology and astrophysics, exploiting the mission unique capability to perform an unprecedented deep monitoring of the soft X-ray transient Universe [14]. Besides high-redshift GRBs, THESEUS will serendipitously detect and localize during regular observations a large number of X-ray transients and variable sources, collecting also prompt follow-up data in the IR. The foreseen payload of THESEUS includes the following instrumentation: Soft X-ray Imager (SXI, 0.3-6 keV), a set of 4 lobster-eye telescopes units, covering a total FOV of 1 sr, with source location accuracy <1-2 arcmin; X-Gamma ray Imaging Spectrometer (XGIS, 2 keV-20 MeV), a set of coded-mask cameras using monolithic X-gamma ray detectors based on bars of Silicon diodes coupled with CsI crystal scintillator, granting a 1.5 sr FOV, a source location accuracy of 5 arcmin in 2-30 keV and an unprecedentedly broad energy band. SXI provides the capability to monitor the X-ray flux of hundreds of AGN with 10% accuracy on daily timescales, and hundreds more on longer timescales. The survey strategy will permit an unbiased look at the long-term variability of an unprecedentedly large AGN/Blazar sample at depths never reached before.

In Table 1 we show a comparison between THESEUS and Chandra capabilities (ACIS-Advanced CCD Imaging Spectrometer; HRC-High Resolution Camera), the last one being the most powerful, up to now, telescope for discovery of X-ray traces in high energy Universe and the first one to observe quasar microlensing caused by FFPs.

***Table 1**. The capabilities of Theseus and Chandra telescopes.*

	Range (KeV)	**FOV**	**Accuracy**	**Sensitivity erg/cm^2/s**
THESEUS SXI/	(0.3 - 6) /	1sr /	10-20 arcsec /	10^{-9} /
Chandra ACIS	(0.4-10)	17x17 arcmin	1 arcsec	$4x10^{-15}$
Theseus XGIS/	(2 KeV –20 MeV)/	1.5sr /	5 arcmin /	10^{-10} /
Chandra HRC	(0.4-10) KeV	30x30 arcmin	0.4 arcsec	10^{-16}

We remark that THESEUS is a unique combination of huge FOV, angular resolution and sensitivity and promises to further on the important discoveries in this direction.

5. Conclusions

The survey strategy of THESEUS will permit an observation of the long-term variability of an unprecedentedly large AGN sample, at depths never reached before. New quasars will be observed, with smaller Einstein Radius of lensing bodies, shorter Einstein times, smaller quasar regions to be probed and closer to the central Black Hole, so with shorter variability.

THESEUS will be characterized by higher sensitivity to study X ray lines (FeKα), which are considered as precious sources of information for different regions of the accretion disk.

Acknowledgements

We acknowledge Tirana University for financing our participation in the conference “The multi-messenger astronomy: gamma-ray bursts, search for electromagnetic counterparts to neutrino events and gravitational waves”. Also, we acknowledge prof. Francesco De Paolis for interesting exchanges during this work.

References

[1] Einstein, A. “Die Grundlage der allgemeinen Relativitätstheorie”, *AnP,* 1916, 354, 769E.

[2] Einstein, A. “On the Influence of Gravitation on the Propagation of Light”, *Ann. Phys*, 1911, 340, 898–908.

[3] Dyson, F.W.; Eddington, A.; Davidson, C. “A determination of the deflection of light by the sun’s gravitational field from observations made at the total eclipse of May 29, 1919”, *Phil. Trans. Roy. Soc. A,* 1920, 220, 291–333.

[4] Einstein, A. “Lens-Like Action of a Star by the Deviation of Light in the Gravitational Field”, *Science,* 1936, 84, 506–507.

[5] Zwicky, F. “On the Probability of Detecting Nebulae which Act as Gravitational lenses”, *Phys. Rev,* 1937, 51, 679–679.

[6] Paczyński, B. “Gravitational microlensing by the galactic halo”, *Astrophys. J.* 1986, 304, 1–5.

[7] Dai, X.; Guerras, E. “Probing Extragalactic Planets Using Quasar Microlensing”, *ApJ.* 2018, 853,

27.

[8] Sumi T. ; et al. “Unbound or Distant Planetary Mass Population Detected by Gravitational Microlensing”, *Nature*, 2011, 473, 349.

[9] Udalski, A.; Szymanski, M.; Kaluzny, J.; et al. “The Optical Gravitational Lensing Experiment”, *AcA*, 1992, 42, 253-284.

[10] Muraki, Y.; Sumi, T.; Abe, F.; et al. “Search for Machos by the MOA Collaboration”, *PThPS*, 1999, 133, 233-246.

[11] Hamolli, L.; De Paolis, F.; Hafizi, M.; Nucita, A.A. “Predictions on the detection of the free-floating planet population with K2 and Spitzer microlensing campaigns”, *AstBu*, 2017, 72 73.

[12] Dong, Subo; Udalski, A.; Gould, A.; et al. “First Space-Based Microlens Parallax Measurement: Spitzer Observations of OGLE-2005-SMC-001”, *Astrophys. J.* 2007, 664, 862.

[13] Zapatero Osorio, M.R.; et al., “Discovery of Young, Isolated Planetary Mass Objects in the σ Orionis Star Cluster”, *Science*, 2000, 290, 103.

[14] Amati, L.; O'Brien, P.; Götz, D.; et al., “The THESEUS space mission concept: science case, design and expected performances”, *AdSpR*, 2018, 62, 191A.

[15] Schneider, P.; Ehlers, G.; Falco, E.E. “Gravitational Lenses”, *Springer Verlag: Berlin, Germany* 1992.

[16] Walsh, D.; Carswell, R.F.; Weymann, R.J. “0957 + 561 A,B: Twin quasistellar objects or gravitational lens?” *Nature*, 1979, 279, 381–384.

[17] Pelt, J.; Kayser, R.; Refsdal, S.; Schramm, T. “The light curve and the time delay of QSO 0957+561”, *Astron. Astrophys*, 1996, 306, 97–106.

[18] Chen, G.H.; Kochanek, C.S.; Hewitt, J.N. “The Mass Distribution of the Lens Galaxy in MG 1131+0456”, *Astrophys. J.* 1995, 447, 62–81.

[19] Browne, I.W.A.; Wilkinson, P.N.; et al. “The Cosmic Lens All-Sky Survey - II. Gravitational lens candidate selection and follow-up”, *Mon. Not. R. Astron. Soc*, 2003, 341, 13–32.

[20] Bolton, A.S.; Burles, S.; Koopmans, L.V.E.; Treu, T.; Moustakas, L.A. “The Sloan Lens ACS Survey. I. A Large Spectroscopically Selected Sample of Massive Early-Type Lens Galaxies”, *Astrophys. J.* 2006, 638, 703–724.

[21] Oguri, M.; Inada, N.; Pindor, B.; Strauss, M.A.; et al. “The Sloan Digital Sky Survey Quasar Lens Search. I. Candidate Selection Algorithm”, *Astrophys. J.* 2006, 132, 999–1013.

[22] Kelly, P.L.; Rodney, S.A.; Treu, T.; Foley, R.J.; et al. “Multiple images of a highly magnified supernova formed by an early-type cluster galaxy lens”, *Science* 2015, 347, 1123–1126.

[23] Tyson, J.A.; Wenk, R.A.; Valdes, F. “Detection of systematic gravitational lens galaxy image alignments—Mapping dark matter in galaxy clusters”, *Astrophys. J.* 1990, 349, L1–L4.

[24] Alcock, C.; et al. “First Observation of Parallax in a Gravitational Microlensing Event”, *ApJ*. 1995, 454, 125.

[25] Dominik, M. “Galactic microlensing with rotating binaries”, *Astron. Astrophys.* 1998, 329, 361.

[26] Hamolli, L. Hafizi, M.; De Paolis, F.; Nucita, A.A. “Paralax effects on microlensing events caused by free-floating planets”, *BlgAJ*. 2013, 19, 34

[27] Witt H. J.; Mao Sh. “Can lensed stars be regarded as pointlike for microlensing by MACHOs?”, *ApJ.* 1994, 430, 505

[28] Hamolli, L. Hafizi, M.; De Paolis, F.; Nucita, A.A. “Estimating Finite Source Effects in Microlensing Events due to Free-Floating Planets with the Euclid Survey”, *Adv. Astron.* 2015 ID 402303

[29] Beaulieu, J.-P.; Bennett, D. P.; et al. “Discovery of a cool planet of 5.5 Earth masses through gravitational microlensing”, *Nature*, 2006, 439, 437B.

[30] Dominik, M.; Sahu, K. C. “Astrometric microlensing of stars”, *ApJ.* 2000, 534, 213.

[31] Nucita, A.A.; et al. “Astrometric microlensing”, *IJMPD.* 2017, 2641015N.

[32] Hamolli, L.; et al. “The astrometric signal of microlensing events caused by free floating planets”, *Ap&SS.* 2018, 363, 153.

[33] Schmidt, R. W.; Wambsganss, J. “Quasar microlensing”, *Gen Relativ Gravit*, 2010, 42, 2127–2150.